Journal of Structural Geology, Vol. 6 No. 3, pp. 273 to 281, 1984
Printed in Great Britain

0191-8141/84 $03.00 + 0.00

The generation of ductile and brittle shear bands in a low-angle mylonite zone

CEES W. PASSCHIER

Department of Geology, University College of Swansea, Swansea, SA2 8PP, U.K.

(*Received* 27 *January* 1983; *accepted in revised form* 15 *September* 1983)

Abstract—In the Saint-Barthélemy Massif, French Pyrenees, a ductile thrust zone developed in gneisses during retrogression from lower amphibolite facies conditions to the upper greenschist facies. The last major structures formed in the zone are isolated shear bands, divided into three types.

Anastomosing, inhomogenous ultramylonitic shear bands (Type I) are subparallel to the mylonitic foliation in the gneiss (S_g). Most of these bands developed by ductile deformation processes only.

Planar, homogeneous ultramylonite bands (Type II) are usually oblique to S_g. They generated as pseudotachylyte bands by brittle fracturing and underwent strong subsequent ductile deformation.

Type III shear bands are planar and oblique to S_g. They consist of pseudotachylyte, weakly affected by ductile deformation.

Type I, II and III bands seem to represent progressively younger structures on a local scale, linked to falling P–T conditions. The systematic variation in orientation of the different shear bands with respect to S_g is interpreted as being due to a different response of brittle and ductile structures to the orientation of the kinematic frame and the rock anisotropy.

INTRODUCTION

THE OCCURRENCE of late zones of concentrated shear strain in domains of non-coaxial ductile deformation has been a subject of interest for a number of years (White 1979, Platt & Vissers 1980, White *et al.* 1980, Passchier 1982a). Microstructurally these zones, called shear bands, show evidence of both brittle and ductile deformation processes (Platt & Vissers 1980). The bands usually form a crenulation and have a consistent orientation with respect to major foliation planes of the rock in which they were formed; they seem to be reliable markers for sense of shear (Platt & Vissers 1980, White *et al.* 1980). Shear bands are thought to be the result of hardening in a mylonite zone (White *et al.* 1980).

This study treats the spatial relationships of several types of major shear bands from a mylonite zone in the Pyrenees. The bands are characterized by wide spacing, strong localization of shear strain and a change of dominant deformation mechanism with age. They represent the final stages of ductile deformation in a major mylonite zone, before it enters the field of dominant brittle fracturing. The microstructural characteristics of these shear bands were treated in an earlier paper (Passchier 1982b).

REGIONAL GEOLOGY

The Saint-Barthélemy Massif is one of the Northern Pyrenean Massifs in France (Fig. 1). It consists of a gneiss core covered by sediments of Palaeozoic age. The gneiss core can be subdivided into a basal unit, probably of Precambrian age, overlain by intrusive and migmatitic gneisses of Variscan age (Zwart 1954, Guchereau 1975, Zwart 1979, Passchier 1982a).

A main structural event of ductile thrusting caused intense deformation in the gneiss (Passchier 1982a). The

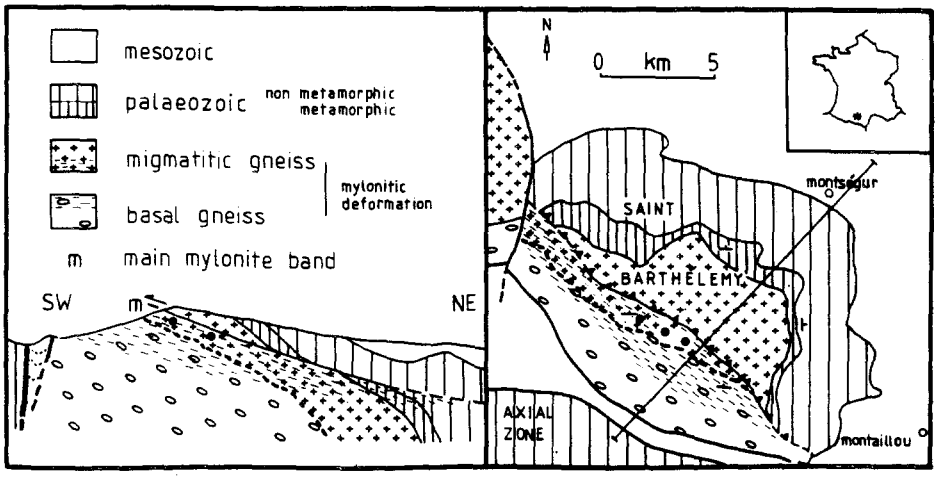

Fig. 1. Simplified map and profile of the Saint Barthélemy Massif based on the maps of Passchier (1982a) and Zwart (1954). Dots—shear band localities.

Table 1. Summary of shear band mesostructures

Type	surface parallel to L_g	surface normal to L_g
I inhomogeneous ultramylonite (oldest bands)	most bands parallel to S_g (Fig. 2a). Some subparallel and less steeply N-dipping	bands parallel to S_g local branching (Fig. 2b)
	individual ultramylonite domains and lenses continuous and planar	individual ultramylonite domains and lenses discontinuous and anastomosing
II homogeneous ultramylonite	most bands oblique to S_g (0–45°, rarely exceeding 30°) most bands less steeply N-dipping than S_g (Figs. 2c, e & g) some bands parallel to S_g	most bands parallel to S_g (Figs. 2d & f) some oblique but angle rarely exceeding 20°
	bands straight—constant thickness	bands undulating—variable thickness
III pseudotachylyte (usually deformed)	orientation as for Type II (Fig. 2j) but more irregular	orientation as for Type II (Figs. 2h & k) but more irregular
(youngest bands)	main bands less straight than Type II; common branching and injection veins	main bands branching; injection veins

result is a well-developed mylonitic shape fabric in the Basal Gneiss unit and in the lower part of the intrusive and migmatitic gneisses, called the Lower Gneiss unit. The upper part, called the Upper Gneiss unit, does not contain well developed deformational fabrics and represents the stable margin of the hanging wall.

The Lower Gneiss unit

The Lower Gneiss unit consists of deformed granodiorite, granite, migmatite, leucogranite and pegmatite. The mylonitic shape fabric in these rocks has well-developed planar (S_g) and linear (L_g) elements. S_g dips gently to the NNE and L_g plunges to the NNW. The shape fabric varies in strength and is best developed where maximum finite strain was reached: in the Main Mylonite Band which is the upper boundary of the Lower Gneiss unit (Fig. 1). The mylonitic fabric developed during retrogression from lower amphibolite facies to upper greenschist facies conditions, as can be demonstrated by sequentially developed parageneses of deformed mineral grains (Passchier 1982a). The age of the ductile thrusting event is as yet uncertain but certainly postdates the peak of Variscan metamorphism.

Microstructurally the shape fabric is defined by the alignment of irregular, virtually monomineralic lenses of dynamically recrystallized quartz, plagioclase, orthoclase, biotite or muscovite mantling old grain remnants. These lenses are surrounded by anastomosing polymineralic aggregates of fine-grained recrystallized quartz, biotite and feldspar. Porphyroclasts of sillimanite, almandine and cordierite are present. Deformation in the gneiss was mainly by ductile deformation and dynamic recrystallization of quartz, biotite and muscovite, and by brittle and ductile deformation of feldspar. Crystallographic preferred orientation fabrics of quartz, dynamic recrystallization of feldspar, the stable co-existence of quartz–biotite–plagioclase–alkali feldspar–mucovite–almandine and the absence of chlorite and epidote indicate upper greenschist facies conditions and low water activity during the final stage of mylonitic deformation in the gneiss (Passchier 1982a). This last is confirmed by the observation that all fluid inclusions in quartz from the Lower Gneiss unit contain CO_2 (Passchier 1982a).

Deformation was strongly non-coaxial, as illustrated by the asymmetry of sense of shear markers, which invariably agree on a movement direction subparallel to L_g, and a southward-directed movement of the hanging wall. Reliable sense of shear markers in the gneiss proved to be: (1) sheath folds in recrystallized aggregates of quartz, feldspar and apatite; (2) trails of recrystallized grains around feldspar and quartz porphyroclasts; (3) folded single quartz grains; (4) lozenge-shaped biotite and muscovite porphyroclasts and (5) a weak shear band cleavage on a centimetre scale.

SHEAR BANDS

Beside the weak shear band cleavage mentioned, a large number of dark, narrow shear bands occur in the upper 300 m of the Lower Gneiss unit in the central part of the area below the Main Mylonite Band (Fig. 1). They define planar fabric elements which dip gently to the N and NE. The bands are usually solitary, often a few hundred m apart. Microstructurally they can be classified as ultramylonite bands, and rarely as pseudotachylyte or ductilely deformed pseudotachylyte bands (Phillpotts 1964, Sibson 1975, 1977, 1980). The bands are most common in the deformed granodiorite and migmatitic gneiss. They sometimes follow lithologic con-

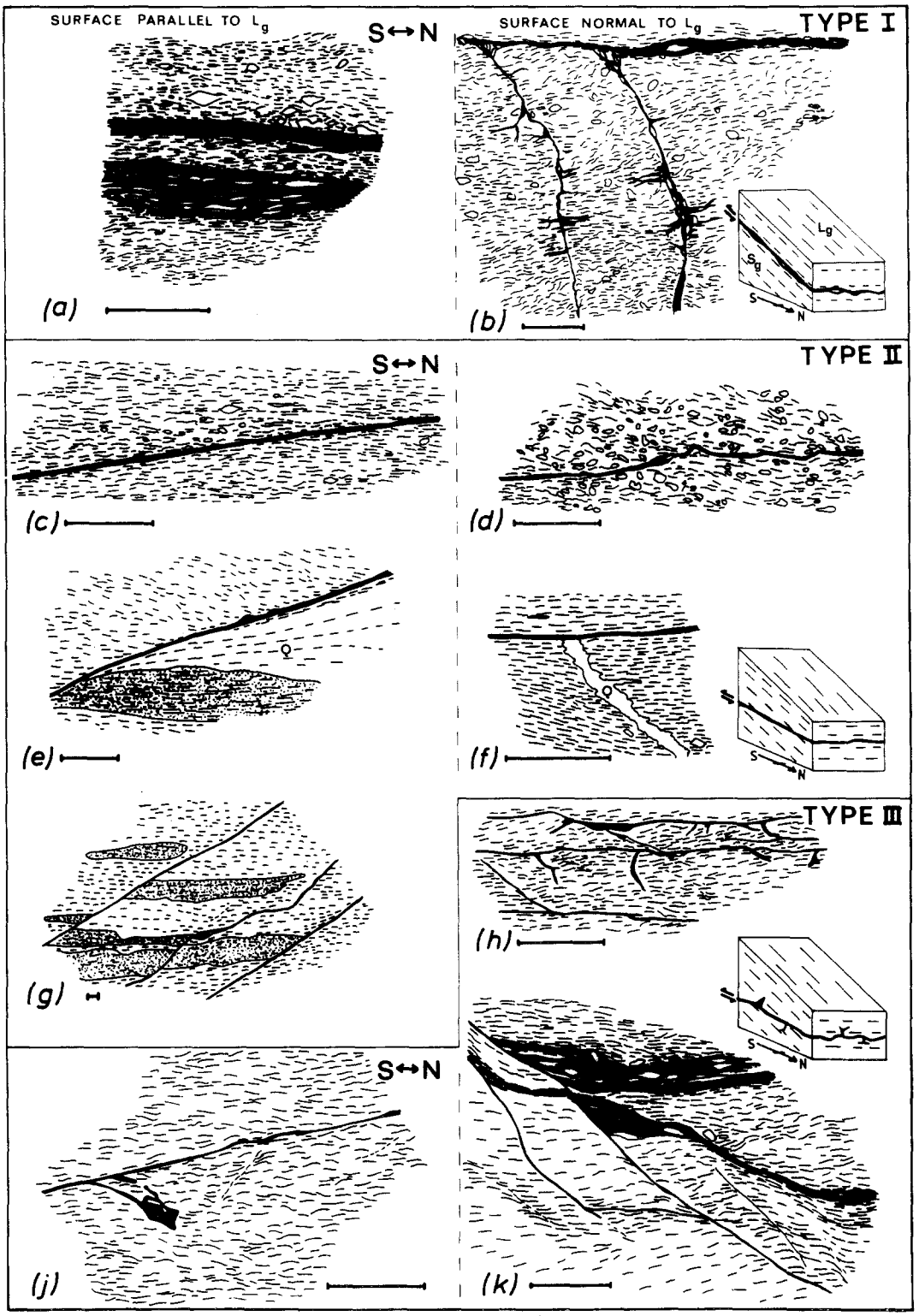

Fig. 2. Profile sketches of different types of shear bands on outcrop surfaces parallel and normal to L_g. Size of scale bar 5 cm. Block diagrams illustrate the most common spatial orientations of the bands. (a) Type I bands subparallel to S_g. (b) Type I band parallel to S_g with irregular branches, locally parallel to S_g. (c) Type II band making a small angle with S_g, which is weakly deflected. (d) Same band on surface normal to L_g. (e) Type II band cutting a quartz lens (Q) and an adjacent amphibolite lens, with deflection of the foliation. (f) Type II band cutting a late weakly deformed quartz vein (Q), which transects S_g. (g) Type II bands cutting xenoliths; smallest displacement and steps parallel to S_g in the central band. The lower band shows deflection of S_g. (h) Type III bands with injection veins. (j) Type III band crosscutting S_g, with an injection vein. (k) Type III bands crosscutting older Type I bands.

tacts between granodiorite and domains of leucogranite, pegmatite, and quartz veins. Although they can occur in many shapes and orientations, three main types of shear band could be distinguished.

Type I

Type I shear bands occur as intensely deformed gneiss in which black or grey ultramylonite lenses and domains

form an anastomosing network (Figs. 2a & b). The bands vary in thickness from 1 cm to 1 m and in length from a few m to several hundreds of m. Individual ultramylonite lenses and domains are 1–10 mm thick and up to 1 m long and have indefinite boundaries. A compositional layering (S_b) and a lineation interpreted as a stretching lineation (L_b) are visible in the field in the individual ultramylonite domains.

The microstructure of ultramylonite in Type I shear bands is inhomogeneous. Abundant porphyroclasts and partially recrystallized lenticular aggregates of quartz, plagioclase, alkali feldspar, biotite, muscovite and other minerals lie in the dark, fine grained matrix (1–10 μm) of quartz, plagioclase and biotite. They define a well-developed compositional layering. Biotite in the matrix has a strong preferred orientation. There is a gradual microstructural transition into the adjoining gneiss (Passchier 1982a).

Type II

In the field, Type II shear bands consist of dark grey or black ultramylonite with a massive, aphanitic appearance and sharp, straight boundaries (Figs. 2c–g). Thickness ranges from 0.1 to 30 mm (usually 1–3 mm) and length from 1 to 100 m. The internal foliation (S_b) and stretching lineation (L_b) are more weakly developed than in ultramylonite of Type I bands. The bands usually cut through the gneiss without abrupt changes in thickness.

Microstructurally Type II bands resemble Type I, but consist dominantly of a homogeneous matrix with few isolated porphyroclasts and lenticular aggregates (Passchier 1982b).

Type III

Type III bands consist of pseudotachylyte or ductilely deformed pseudotachylyte (Phillpotts 1964, Sibson 1975, 1980). They occur as narrow, straight main bands, up to a few mm thick, from which veins of a dark aphanitic material run into the surrounding gneiss (injection veins, Figs. 2h & j). The main bands resemble Type II shear bands but have a more irregular thickness and orientation (Passchier 1982a, 1982b). Only in ductilely deformed main bands can an internal foliation and a stretching lineation (L_b) be observed. Passchier (1982b) describes the microstructure.

MESOSTRUCTURE OF SHEAR BANDS

Nearly 250 shear bands of various types were mapped in detail. Most observations were made on vertical outcrop walls and, since most bands are flat-lying, these data allow reconstruction of their three dimensional shape and orientation. It was found convenient to divide observations into those made on surfaces normal to L_g and parallel to L_g. The data are summarized in Table 1. The following general statements can be made:

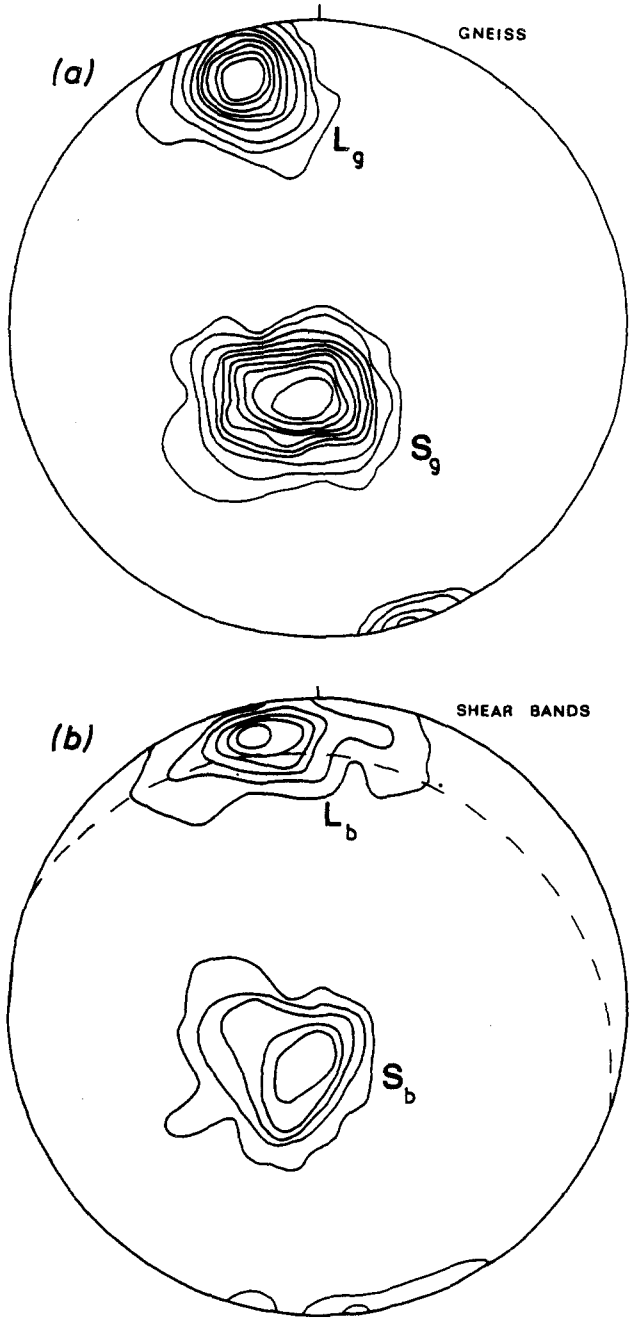

Fig. 3. Contoured diagrams showing the orientation of: (a) stretching lineations (L_g—163 measurements) and poles to the mylonitic foliation (Sg—292 measurements) in gneiss of the Lower Gneiss unit; (b) stretching lineations in shear bands (L_b—141 measurements) and poles to the bands (S_b—248 measurements). Great circle indicates mean orientation of the mylonitic foliation (S_g). Equal-area projections. Contour interval 5 measurements per 1% area.

(1) On a regional scale S_g and the shear bands have strongly overlapping orientation fields, but the bands have a more scattered pattern. The same applies to the orientations of L_g and L_b (Fig. 3).

(2) In outcrop, shear bands have a consistent orientation with respect to S_g (Table 1). Type I bands are usually sub-parallel to S_g, while Type II and Type III bands tend to cross cut S_g with constant sense, the shear bands dipping less steeply northward than S_g. Many bands which are oblique to S_g show steps, where the band trends parallel to S_g for short stretches (e.g. Fig. 2g). These steps occur on a scale of 1 cm to tens of cm.

(3) Type I and Type II shear bands are narrow zones of non-coaxial ductile deformation. This follows from the microstructure (Passchier 1982b), the displacement of markers and the deflection of S_g along the bands (Figs. 2c & e). Type III bands generated as pseudotachylyte by melting of the rock on a seismically active fault, and underwent little ductile deformation (Passchier 1982b). Type II and some Type I bands were probably generated in the same way as Type III bands, but most strain in the bands was ductile, post-dating the brittle event (Passchier 1982a, 1982b). At least some Type I bands were entirely formed by ductile deformation processes. Since no evidence for volume change along the bands was found, their shape implies that the ductile deformation had a very large simple shear component.

(4) Displacement along the bands was sub-parallel to L_g with the same sense of movement on 98% of the major bands investigated; that is a southward-directed movement of the hanging wall, similar to the sense of movement in the major shear zones and in the host gneiss. This is indicated by (*a*) the sense of deflection of S_g along bands on surfaces parallel to L_g (Figs. 2c & e); (*b*) the absence of deflection of S_g along bands on surfaces normal to L_g; (*c*) the offset of markers such as xenoliths, feldspar augen, quartz lenses and gneissic layering sub-parallel to L_g (Figs. 2e & g); (*d*) the asymmetry of microstructures in the bands (Passchier 1982a); (*e*) the variable attitude of shear bands on surfaces parallel and normal to L_g (Fig. 2 and Table 1).

(5) Five Type II shear bands yielded a northward-directed movement of the hanging wall. These bands dip more steeply northward than S_g and probably represent local backthrusting without regional significance.

(6) The amount of displacement along a shear band seems to increase with its thickness. A maximum displacement of several m has been observed for some Type II bands (Fig. 2g). The amount of displacement seems to be larger on Type II bands than on Type I or Type III bands.

(7) Type III bands commonly branch in an irregular way indicating that lateral displacement along them must have been small (Fig. 4a). This is in contrast with branches along Type I bands, which tend to be sub-parallel to L_g and contain a stretching lineation of the same orientation as L_b in the main band (Fig. 4b); they probably accommodated local inhomogeneities in the shear strain distribution around the main band.

(8) Shear bands are believed to have formed during the last stage of the ductile thrusting event which caused development of the mylonitic shape fabric in the gneiss. The presence of this shape fabric and the lens or rod shape of deformed xenoliths are indicative of extensive ductile deformation. The shear bands cut S_g and the deformed xenoliths sharply and are never overprinted by younger mylonitic effects. Figure 2(f) shows a weakly deformed quartz vein which cuts S_g and is cut by a Type II shear band. The orientations of the stretching lineations L_g and L_b are very similar, and sense of shear in the bands is identical to that in the gneiss.

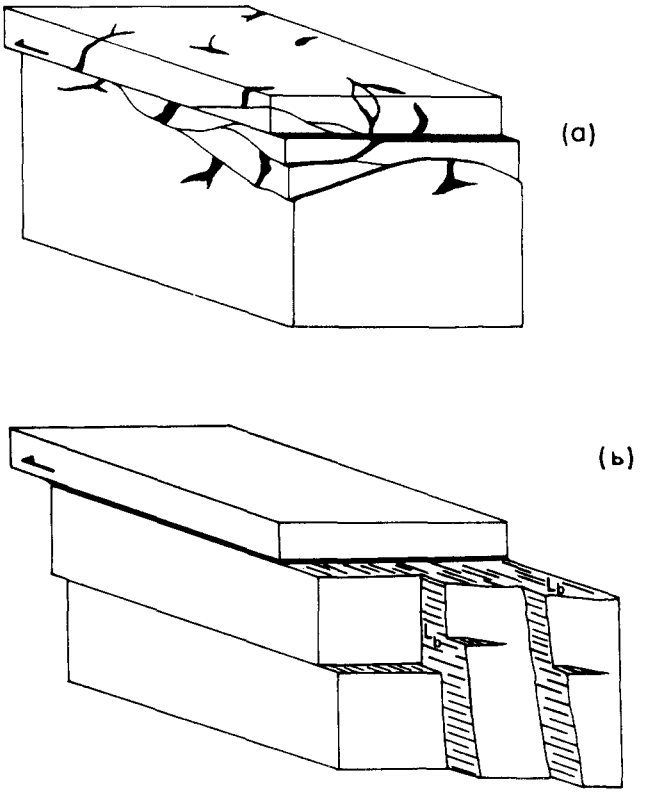

Fig. 4. (a) Schematic diagram of brittle displacement along a Type III shear band. No displacement occurs along injection veins, and amount of displacement along the irregularly oriented branches is small. (b) Schematic diagram of ductile displacement along a Type I shear band and associated branches; L_b is subparallel to the flow direction, and all branches are parallel to L_b.

KINEMATIC SIGNIFICANCE OF SHEAR BANDS

The development of shear bands as a last stage of the ductile thrusting event may reflect changes in the rheological behaviour of the rock or changes in the kinematic framework imposed upon the rock. Only the former effect seems to be important in the Saint-Bathélemy Massif (see below). Changes in stable mineral parageneses, in microstructures produced and in density of CO_2 fluid inclusions indicate locally falling P–T conditions contemporaneous with the ductile thrusting event, leading to an increase in strain hardening. This is attributed to synkinematic uplift of the mylonite zone and rapid erosion, although the presence of relatively cool rocks in the hanging wall may have strengthened the effect (Passchier 1982a).

Abundant data support the view that non-coaxial ductile deformation in rocks tends to become restricted to increasingly narrow zones with increasing hardening of the rock (Nicolas & Poirier 1976, Poirier 1980, White *et al.* 1980). This apparently minimizes the elastic potential energy of the rock and the rate of energy dissipation as heat (Lister & Williams in press). In the same way the presence of pseudotachylyte cutting mylonitic fabrics can be explained by increasing strength of the rock, but at rather restricted metamorphic and kinematic conditions. It develops after most ductile deformation in the rock has ceased, at lower P–T conditions than ductile

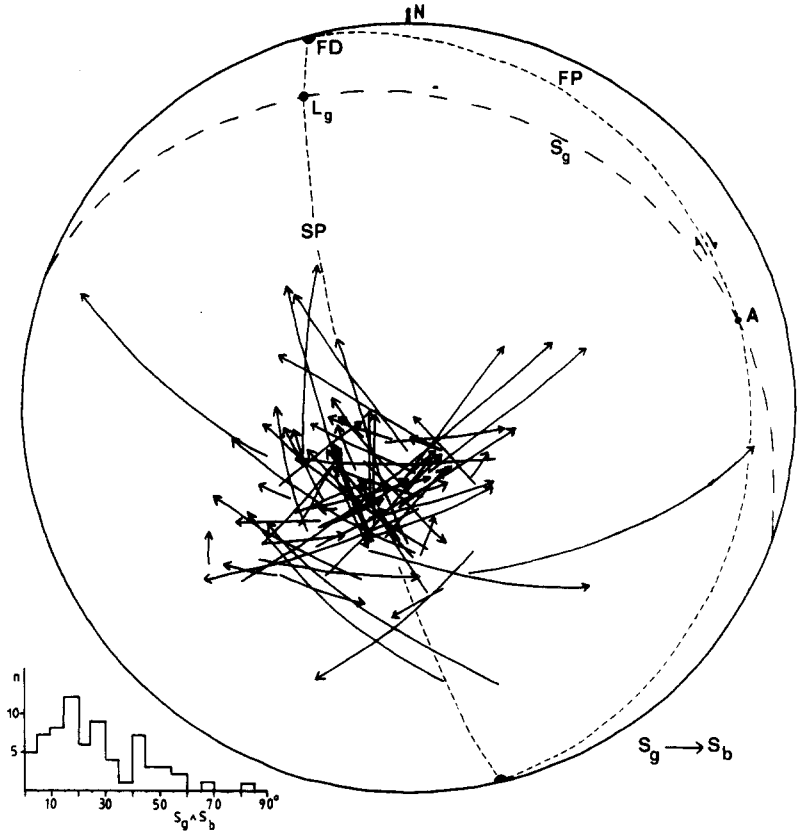

Fig. 5. Orientation pairs, in single outcrops, of shear bands (S_b) and S_g in the adjacent gneiss. Poles to S_g and S_b are indicated by the base and head of an arrow, respectively, and the angle between them plotted in a histogram. Mean values of S_g and L_g, from Fig. 3, are indicated. FD and FP are the inferred flow direction and flow plane of the kinematic frame of shear band generation, based on a 10° angle between S_g and the flow plane in the symmetry plane (SP) of the material frame. Further explanation in text.

shear zones (Park 1961, Francis & Sibson 1973, Sibson 1977, Allen 1979, Grocott 1981).

In the Lower Gneiss unit a decrease of shear zone width and subsequent generation of pseudotachylyte is clearly observed. Where shear bands are seen to intersect, Type I bands are cut by Type II or III (Fig. 2k). Fluid inclusion data indicate that CO_2 inclusions associated with Type I bands have a higher density than those associated with Type III, indicating that the latter are younger in a retrograde metamorphic system: inclusions associated with a Type I band indicate 2.5–3 kbar at 450–550°C (upper greenschist facies) and those associated with a Type III band approximately 2 kbar in the same temperature range (Passchier 1982a). If these stress estimates are near the mean stress, a depth of formation of 8–9 km for Type I and 5–6 km for Type III bands can be postulated.

Thus, the shear bands fit in a sequence of generally decreasing ductility, from concentration of ductile deformation in Type I bands to pseudotachylyte generation when the mean stress had sufficiently decreased. The first-formed pseudotachylyte bands were strongly deformed to Type II, and rarely to Type I, bands; those formed at a later stage were more weakly deformed, insufficiently to erase pseudotachylyte microstructures (Type III). Nevertheless, the actual difference in age may be relatively small and different types of bands may have formed contemporaneously at different locations and depths in the gneiss.

ORIENTATION OF SHEAR BANDS

Figure 3 illustrates that a considerable scatter in orientation, both of S_g and of shear bands, exists over the area. The angular relationship of S_g and the shear bands is not random, however. For oblique shear bands, the orientations of S_g and the bands were measured in 69 locations, and the two poles in each case were plotted and joined by an arrow to indicate the angular relationship (Fig. 5). The arrows tend to point outwards from S_g poles with a strong affinity for the NW and NE quadrants, and an angle of 15–20° between $S_g$and shear bands is most common. This is in accordance with field observations of a constant angular relationship of $S_g$and the bands on surfaces parallel to L_g (Fig. 2 and Table 1). A possible explanation for these observations is a strict confinement of the orientation of both S_g and the shear bands to the orientation of the kinematic frame of mylonitic deformation. Since the orientation of the kinematic frame may have varied from place to place, the orientations of S_g and shear bands will have developed a corresponding regional variation, causing an overlap in their orientation patterns. The scatter in the directions of arrows in Fig. 5 can be similarly explained.

Type I shear bands are commonly parallel to S_g, while Type II and III make an angle with it. This effect could be due to a change in the orientation of the kinematic frame with time, or to a different response of ductile and

brittle shear bands to the rock anisotropy and an invariable orientation of the kinematic frame. Possible reorientations of the kinematic frame are restricted by the fact that mean orientations of L_g and L_b do not differ significantly (Fig. 3), and by the absence of a clear asymmetry in the orientation pattern of arrows in Fig. 5 with respect to the symmetry plane (SP) of the material frame of S_g and L_g. Therefore, the only possible reorientation of the kinematic frame is in the dip of the flow plane around axis 'A'. This means that the model can be simplified to two dimensions in plane 'SP' (Fig. 5).

Anisotropy of the gneiss had a noticeable influence on the orientation of shear bands. This is apparent from the occurrence of steps parallel to S_g in inclined bands (Figs. 2g & k) and of branches parallel to S_g (Fig. 2b). Probably the elongate distribution pattern of L_b parallel to the mean orientation of S_g is also an effect of the anisotropy (Fig. 3).

Many authors have reported that the angle between the direction of maximum rate of shortening and a shear zone is smaller for brittle zones than for ductile ones in the same rock at a fixed orientation of the kinematic frame (Cobbold *et al.* 1971, Ramsay & Allison 1979, Ramsay 1980). The same seems to apply to the Saint-Barthélemy Massif. Therefore the effect of the orientation of the kinematic frame and the anisotropy of the rock on the orientation of developing shear bands must be investigated, making a clear distinction between those bands generated as brittle fractures and those generated as ductile structures.

Ductile shear bands

The Type I bands which formed without a pseudotachylyte stage probably developed by local enhanced strain softening in the mylonite zone. After an initial stage of mainly intracrystalline deformation in quartz, feldspar and micas, falling P–T conditions led to hardening of quartz and feldspar and accompanying dynamic recrystallization to smaller grain sizes (Passchier 1982a,b). This favoured grain boundary sliding or continuous dynamic recrystallization in fine-grained polymineralic aggregates of feldspar, white mica and biotite, both deformation mechanisms with a low yield strength and small strain hardening effects (Boullier & Gueguen 1975, Post 1977, White *et al.* 1980, Zeuch 1983). The 'soft' aggregates were hampered in attracting all ductile shear strain due to the stress supporting framework of rigid elements in the rock. Locally, large lensoid aggregates of soft material may have developed sufficiently high differential stresses around their tips to enhance grain size reduction and cause lateral growth, comparable to the growth of a dislocation loop in a crystal (e.g. Benioff 1964, Nicolas & Poirier 1976, Ball 1980). This may have produced a large enough volume of fine grained material to further concentrate ductile deformation, developing a Type I band in the process (Fig. 6a).

The lensoid aggregates of relatively soft, fine-grained material are part of S_g. The angle between S_g and the local orientation of the flow plane of the kinematic frame

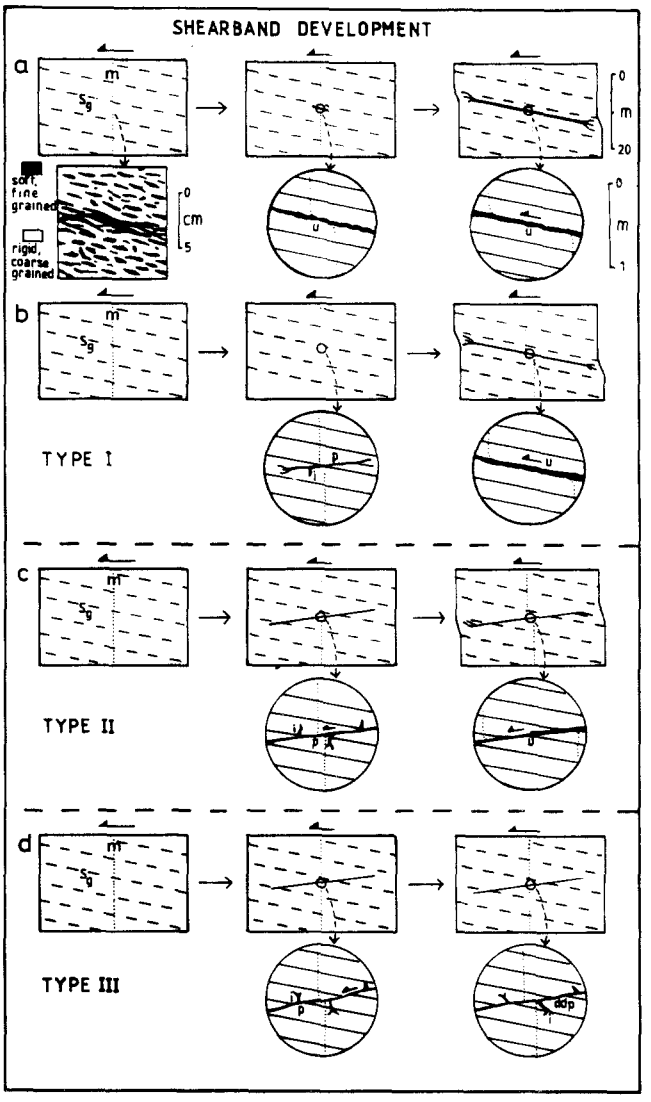

Fig. 6. Schematic representation of the development of different types of shear bands in the mylonitized gneiss in cross sections parallel to the flow direction. (a) Development of a Type I band by enhanced dynamic recrystallization and lateral growth in the host gneiss. (b) Development of a Type I band from a small crystallized pseudotachylyte nucleus by lateral growth due to enhanced recrystallization at its tips. (c) and (d) Ductile regeneration of large pseudotachylyte bands with limited lateral growth, developing into Type II bands (large ductile strain) or Type III bands (small ductile strain). p, pseudotachylyte; i, injection vein; u, ultramylonite; m, shear strain marker.

at the start of ductile shear band generation must have been smaller than 15°, since deformation was strongly non-coaxial; no evidence for volume change was found and shear strains usually exceed $\gamma = 3$ in the mylonitized gneiss. Shear strain values may be found from deformed xenoliths and the orientation of S_g with respect to the trend of the stable margin of the hanging wall (Ramsay & Graham 1970). For these reasons the orientation of S_g, that is of the soft, fine-grained aggregates, approached a direction of maximum shear strain rate (Figs. 6a and 7). This may explain the preferential development of Type I shear bands subparallel to S_g (cf. Platt & Vissers 1980).

In some cases small cores of crystallized early pseudotachylyte may have acted as relatively large lenses of soft material, resulting in the development of a Type I shear band by ductile lateral growth (Fig. 6b).

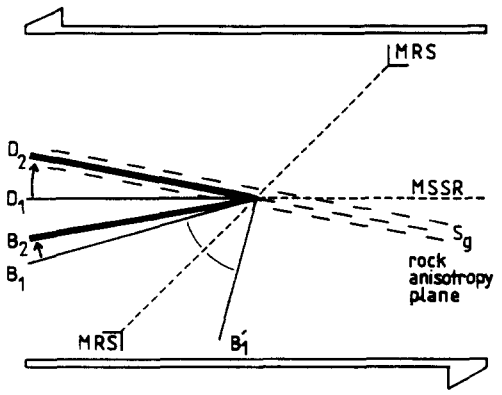

Fig. 7. Orientation of shear bands with respect to the rock anisotropy plane and elements of the kinematic frame of mylonitic deformation on a surface parallel to the flow direction. D_1, ductile shear zone in isotropic rock; D_2, ductile shear zone propagated along material planes in anisotropic rock (Type I); B_1 and B_1', Navier–Coulomb brittle fractures in isotropic rock; B_2, modified Navier–Coulomb brittle fracture in anisotropic rock (Type II, III). MRS, direction of maximum rate of shortening; MSSR, direction of maximum shear strain rate. $S_g \Lambda$ MSSR = 10°, based on finite strain measurements. $S_g \Lambda B_2$ = 20°, based on Fig. 5.

Brittle shear bands

Large pseudotachylyte bands that were generated by brittle fracturing during the last stage of the ductile thrusting event developed into Type II bands by ductile regeneration, probably with limited lateral growth (Fig. 6c); where ductile regeneration was weak they developed into Type III bands (Fig. 6d).

Donath (1961) and Jaeger (1969) state that the Navier–Coulomb criterion of brittle fracturing, which implies that the direction of the compressive stress must lie in the acute angle between a pair of conjugate shear faults, should be modified for anisotropic rocks. Only one of the conjugate shear fractures will form in this case, that is the one nearest to the plane of the anisotropy (S_a). The orientation of this fracture will lie between S_a and the orientation predicted by the Navier–Coulomb criterion for isotropic rocks. The magnitude of the rotation of the potential fracture plane depends on the strength of the anisotropy and the angle between S_a and σ_1 (Jaeger 1969). In strongly anisotropic rocks like slates, the effect can be for fractures to follow S_a for values of $S_a \Lambda \sigma_1$ up to 30°, but for a weak anisotropy as in the Lower Gneiss unit the effect is probably less (Donath 1961).

In the Saint-Barthélemy Massif, brittle shear bands (Type II and III) usually developed after ductile ones in any one area. Figure 7 illustrates that at an invariable orientation of the flow plane of the kinematic frame during the entire mylonitic event, brittle shear bands could be expected to show the orientation with respect to S_g actually observed. Uncertainties in the orientation of σ_1 and the kinematic frame, and possible changes in the original angle due to superimposed accommodative strains such as reverse drag (Platt & Vissers 1980), make accurate predictions difficult. Nevertheless, the difference in generation mechanism between ductile and brittle shear bands seems sufficient to explain the observed variations in shear band orientation without having to postulate a change in orientation of the kinematic frame with time.

CONCLUSIONS

(1) Shear bands developed as the final deformation products in an uplifted low-angle mylonite zone at relatively high local temperature.

(2) The different properties of three distinguishable types of shear band can be explained from their different relative age and generation mechanism.

(3) The orientations of shear bands with respect to S_g can be explained by the change in effect of rock anisotropy for different mechanisms of shear band generation: a change in orientation of the kinematic frame with time is not necessary to explain the data.

Acknowledgements—The author thanks J. Grocott, N. Fry, R. Graham and other colleagues in Swansea for offering valuable suggestions.

REFERENCES

Allen, A. R. 1979. Mechanism of frictional fusion in fault zones. *J. Struct. Geol.* **1**, 231–243.

Ball, A. 1980. A theory of geological faults and shear zones. *Tectonophysics* **61**, T1–T5.

Benioff, H. 1964. Earthquake source mechanisms. *Science* **143**, 1399–1406.

Boullier, A. M. & Gueguen, Y. 1975. SP-Mylonites: origin of some mylonites by superplastic flow. *Contr. Miner. Petrol.* **50**, 93–104.

Cobbold, P. R., Cosgrove, S. W. & Summers, J. M. 1971. Development of internal structure in deformed anisotropic rocks. *Tectonophysics* **12**, 23–54.

Donath, F. A. 1961. Experimental study of shear failure in anisotropic rocks. *Bull. geol. Soc. Am.* **72**, 985–990.

Francis, P. W. & Sibson, R. H. 1973. The Outer Hebrides Thrust. In: *The Early Precambrian of Scotland and Related Rocks of Greenland* (edited by Park, R. G. & Tarney, J.). Univ. of Keele, 95–104.

Grocott, J. 1981. Fracture geometry of pseudotachylyte generation zones: a study of shear fractures formed during seismic events. *J. Struct. Geol.* **3**, 169–179.

Guchereau, J. Y. 1975. Le Saint-Barthélemy metamorphique: petrographie et structure. Unpublished Ph.D. thesis, University of Toulouse.

Jaeger, J. C. 1969. *Elasticity, Fracture and Flow*. Methuen, London.

Lister, G. S. & Williams, P. F. in press. The partitioning of deformation in flowing rock masses. *Tectonophysics*.

Nicolas, A. & Poirier, J. P. 1976. *Crystalline Plasticity and Solid State Flow in Metamorphic Rocks*. Wiley, New York.

Park, R. G. 1961. The pseudotachylyte of the Gairloch District, Ross-shire, Scotland. *Am. J. Sci.* **259**, 542–550.

Passchier, C. W. 1982a. Mylonitic deformation in the Saint-Barthélemy Massif, French Pyrenees, with emphasis on the genetic relationship between ultramylonite and pseudotachylyte. GUA Papers of Geology, Series 1, **16**, 1–173.

Passchier, C. W., 1982b. Pseudotachylyte and the development of ultramylonite bands in the Saint-Barthélemy Massif, French Pyrenees. *J. Struct. Geol.* **4**, 69–79.

Phillpots, A. R. 1964. Origin of pseudotachylytes. *Am. J. Sci.* **262**, 1008–1035.

Platt, J. P. & Vissers, R. L. M. 1980. Extensional structures in anisotropic rocks. *J. Struct. Geol.* **2**, 397–410.

Poirier, J. P. 1980. Shear localization and shear instability in materials in the ductile field. *J. Struct. Geol.* **2**, 135–142.

Post, R. L. Jr. 1977. High-temperature creep of Mt. Burnet dunite. *Tectonophysics* **42**, 75–110.

Ramsay, J. G. 1980. Shear zone geometry: a review. *J. Struct. Geol.* **2**, 83–101.

Ramsay, J. G. & Graham, R. H. 1970. Strain variation in shear belts. *Can. J. Earth Sci.* **7**, 786–813.
Ramsay, J. G. & Allison, I. 1979. Structural analysis of shear zones in an alpinised Hercynian granite. *Schweiz. miner. petrogr. Mitt.* **59**, 251–279.
Sibson, R. H. 1975. Generation of pseudotachylyte by ancient seismic faulting. *Geophys. J. R. astr. Soc.* **43**, 775–794.
Sibson, R. H. 1977. Fault rocks and fault mechanisms. *J. geol. Soc. Lond.* **133**, 191–213.
Sibson, R. H. 1980. Transient discontinuities in ductile shear zones. *J. Struct. Geol.* **2**, 165–174.
White, S. 1979. Large strain deformation: report on a Tectonic Studies Group discussion meeting held at Imperial College, London. *J. Struct. Geol.* **1**, 333–339.
White, S., Burrows, S. E., Carreras, J., Shaw, N. D. & Humphreys, F. J. 1980. On mylonites in ductile shear zones. *J. Struct. Geol.* **2**, 175–187.
Zeuch, D. 1983. On the interrelationship between grain size sensitive creep and dynamic recrystallization of olivine. *Tectonophysics* **93**, 151–168.
Zwart, H. J. 1954. La géologie du massif du Saint-Barthélemy, Pyrénées, France. *Leid. geol. Meded.* **18**, 1–288.
Zwart, H. J. 1979. The geology of the central Pyrenees. *Leid. geol. Meded.* **50**, 1–74.